

**QA Verification of Computer Codes
Used in ORNL/TM-1999/159**

**P. T. Williams
B. R. Bass**

**QA Verification of Computer Codes
Used in ORNL/TM-1999/159**

P. T. Williams

B. R. Bass

Computational Physics and Engineering Division

Manuscript Completed – February 2000

Date Published – March 2000

**Prepared by the
OAK RIDGE NATIONAL LABORATORY
Oak Ridge, Tennessee 37831-8056
managed by
LOCKHEED MARTIN ENERGY RESEARCH CORP.
for the
U. S. DEPARTMENT OF ENERGY
under Contract No. DE-AC05-96OR22464**

CONTENTS

	<u>Page</u>
LIST OF FIGURES	iv
ABSTRACT	v
1. INTRODUCTION.....	1
2. COMPUTER SYSTEMS AND CODES USED IN THE PREPARATION OF ORNL/TM-1999/159.....	2
3. QA STATUS OF CODES.....	3
3.1 ORNOZL	3
3.2 ABAQUS/STANDARD.....	3
4. QA VERIFICATION CALCULATIONS.....	4
4.1 ABAQUS VERIFICATION BENCHMARK.....	4
4.2 ORNOZL/ABAQUS VERIFICATION BENCHMARK.....	6
5. CONCLUSIONS.....	9
REFERENCES	10
APPENDIX A: ORNOZL Output file (NOZZLE – I) Case Run: 11 February, 2000.....	11
APPENDIX B: ORNOZL Output file (NOZZLE – II) Case Run: 11 February, 2000.....	14
APPENDIX C: MATHCAD DATA SHEETS WITH EVALUATION OF APPROXIMATE STRESS-INTENSITY FACTORS USING THE GUZHONG AND QICHAO (1990) APPROXIMATION	17

LIST OF FIGURES

<u>Figure</u>		<u>Page</u>
Fig. 1.	Listing of all files on the archival CD for ORNL/TM-1999/159.	2
Fig. 2.	ORNOZL-generated finite-element models for (a) nozzle-I and (b) nozzle-II configurations using input data from Example Problems I and II in Ref. [4].....	3
Fig. 3.	ABAQUS verification problem: linear-elastic stress-intensity factor for semi-elliptic surface flaw in a semi-infinite medium (a) Mode I tensile loading of surface flaw and (b) benchmark comparison with Newman-Raju solution.	4
Fig. 4.	Geometry of nozzle-corner flaw.....	7
Fig. 5.	Comparison of ABAQUS solutions to predictions of Guozhong and Qichao (1990).....	8

ABSTRACT

This report describes QA verification exercises carried out for the computer codes applied in the analyses summarized "Stress Intensity Factors for HFIR HB-2 Nozzle Corner" (ORNL/TM-1999/159). Several benchmark problems are presented that establish the following: (1) The version of the finite-element mesh generator code ORNOZL used in the subject analyses reproduces the results of the two sample problems given in its previously published user's guide. (2) The ABAQUS code reproduces, independently of ORNOZL, the results of a benchmark verification problem given in its Example Problems Manual that compares linear-elastic stress intensity factors for semi-elliptical surface flaws to solutions published in the literature. (3) The ORNOZL/ABAQUS code combination was benchmarked against an approximate method for estimating linear-elastic stress-intensity factors for corner flaws in pressure vessel nozzles. In addition, all input and output files produced during the analyses described in ORNL/TM-1999/159 have been archived on an electronic medium (CD-R74-ORNL/TM-1999/159) and transmitted with this report to ORNL Research Reactors Division personnel for archival storage.

1. INTRODUCTION

In support of probabilistic fracture mechanics (PFM) studies for the High Flux Isotope Reactor (HFIR) Vessel Life Extension Program [1], a report entitled “Stress Intensity Factors for HFIR HB-2 Nozzle Corner,” (ORNL/TM-1999/159) [2] was recently issued that presented the results of stress analyses of the HFIR HB-2 beam tube in which linear-elastic fracture mechanics (LEFM) stress intensity factors for postulated corner flaws were calculated. The study described in ORNL/TM-1999/159 employed two computer codes: (1) the ORNOZL mesh generation code and (2) the ABAQUS stress-analysis code. This report provides supporting documentation of QA verification for these two codes.

3. QA STATUS OF CODES

3.1 ORNOZL

The ORNOZL finite-element mesh generation code was developed at ORNL in support of the US Nuclear Regulatory Commission (USNRC) sponsored Heavy Section Steel Technology (HSST) Program. The code's user's guide was documented in a USNRC NUREG report [4] which underwent internal ORNL peer review and USNRC review. The two test cases reported in [4] were rerun for this study and checked against the output listings given in ref. [4] (see Fig. 2 and Appendices A and B). The results of this check established that the current copy of ORNOZL reproduces the same output file as the code documented in 1992. The results of additional QA verification calculations are presented in Sect. 4.

3.2 ABAQUS/STANDARD

The developers of ABAQUS, (Hibbit, Karlson, and Sorenson, Inc., (HKS)) have implemented a Quality Assurance Plan that is based on the ANSI/ASME NQA-1 Quality Assurance standard, which is designed to ensure compliance with Appendix B of US federal regulation 10 CFR 50 (1-1-86), *Quality Assurance Criteria for Nuclear Power Plants and Fuel Reprocessing Plants*. HKS contracts annually with an independent quality assurance audit organization to audit HKS's quality assurance procedures. The audit organization is chosen for its experience and its ability to ensure that HKS complies with the provisions of the ISO 9001:1994 and NQA-1 quality standards. ABAQUS is certified under ISO 9001 Certificate No. A3897 issued by the Underwriters Laboratory, Inc.[®] (issue date: April 9, 1996; revision date: March 9, 1998; renewal date: April 9, 2000).

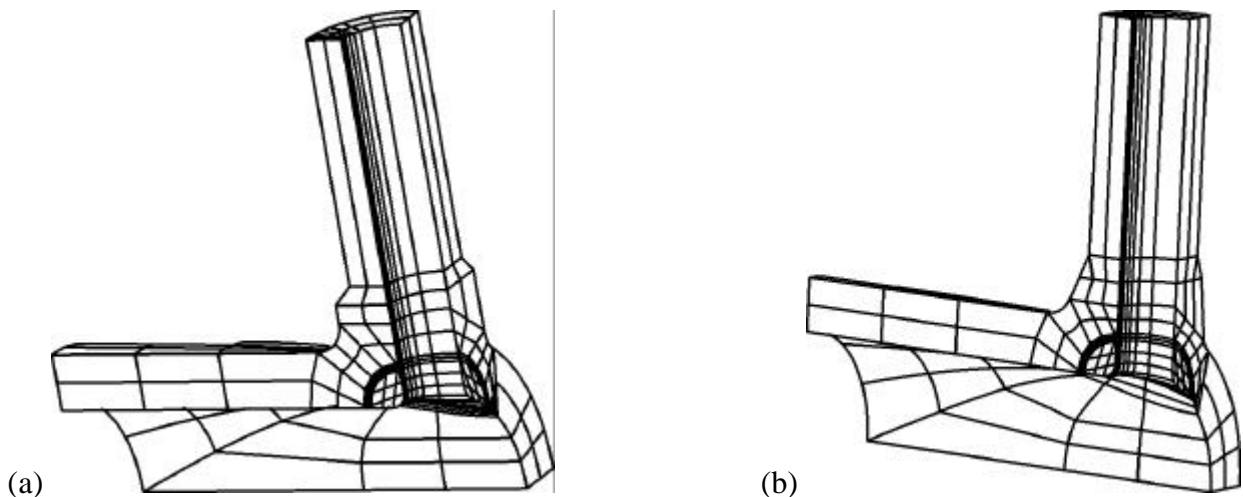


Fig. 2. ORNOZL-generated finite-element models for (a) nozzle-I and (b) nozzle-II configurations using input data from Example Problems I and II in Ref. [4]

4. QA VERIFICATION CALCULATIONS

4.1 ABAQUS Verification Benchmark

Example Problem 3.1.7 in ref. [5] presents, as a verification benchmark, a comparison of stress intensity factors calculated from ABAQUS-generated J -integral results with linear-elastic stress-intensity factors using the correlations developed by Newman and Raju in ref. [6] for a semi-elliptic surface flaw in a semi-infinite medium under a Mode I tensile loading (see Fig. 3). The J -integrals calculated by ABAQUS are converted into stress-intensity factors, K_J , using the following plane-strain relation

$$K_J = + \sqrt{\left(\frac{E}{1-\nu^2}\right) J} \quad (1)$$

The J -integrals generated with the current check calculation are compared in Table 1 to the J -integral estimates published in ref. [5]. The comparison shows that the current study using ABAQUS reproduces the ABAQUS J -integral results reported in ref. [5], and there is good agreement between ABAQUS and the Newman-Raju [6] solution with the discrepancies in the results increasing as the flaw front approaches the free surface at $\phi = 0$. As discussed in [5], the accuracy loss near the free surface is assumed to be attributable to the coarse and rather distorted mesh in this region.

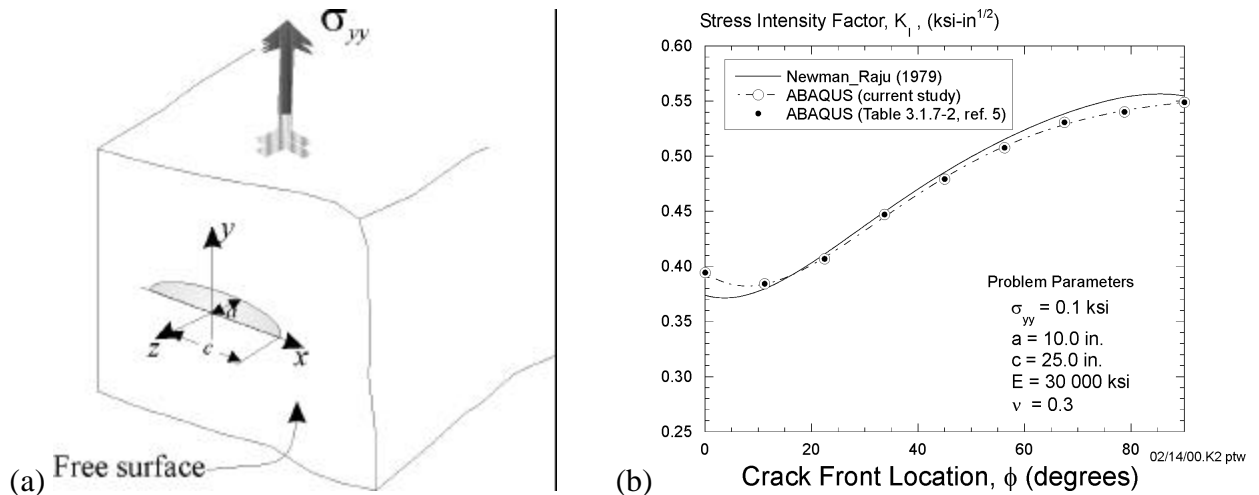


Fig. 3. ABAQUS verification problem: linear-elastic stress-intensity factor for semi-elliptic surface flaw in a semi-infinite medium (a) Mode I tensile loading of surface flaw and (b) benchmark comparison with Newman-Raju solution.

Table 1. Comparison of Current ABAQUS Solution to Table 3.1.7-1 in Ref. [5]

Crack Front Location (degrees)	Current ABAQUS J -integral estimates (lbf-in./in. ²)				J -integral estimates from Table 3.1.7-1 in [5] (lbf-in./in. ²)			
	Contour 1	Contour 2	Contour 3	Average Value	Contour 1	Contour 2	Contour 3	Average Value
0.00	0.0047447	0.0046331	0.0047847	0.0047208	0.0047447	0.0046331	0.0047847	0.0047208
11.25	0.0043670	0.0045162	0.0045531	0.0044788	0.0043670	0.0045162	0.0045531	0.0044787
22.50	0.0051080	0.0050077	0.0049506	0.0050221	0.0051080	0.0050077	0.0049506	0.0050223
33.75	0.0060384	0.0060625	0.0060953	0.0060654	0.0060384	0.0060625	0.0060953	0.0060656
45.00	0.0069947	0.0069676	0.0069397	0.0069673	0.0069947	0.0069676	0.0069397	0.0069673
56.25	0.0078177	0.0078212	0.0078161	0.0078183	0.0078177	0.0078212	0.0078161	0.0078183
67.50	0.0085532	0.0085439	0.0085435	0.0085469	0.0085532	0.0085439	0.0085435	0.0085467
78.75	0.0088540	0.0088523	0.0088484	0.0088516	0.0088540	0.0088523	0.0088484	0.0088516
90.00	0.0091341	0.0091367	0.0091483	0.0091397	0.0091341	0.0091367	0.0091483	0.0091397

4.2 ORNOZL/ABAQUS Verification Benchmark

The combination of the ORNOZL/ABAQUS codes used to produce finite-element solutions of stress-intensity factors for nozzle corner flaws has been benchmarked against an approximate method presented by Guozhong and Qichao [7]. In ref. [7], the iso-stress lines at a nozzle corner are simplified into slanted straight lines at an angle of 45° with the walls of a cylindrical pressure vessel and nozzle. In this approximation, nozzle corner cracks are represented by simplified quarter-circular flaws. The vessel geometry, nozzle geometry, and associated nomenclature are depicted in Fig. 4. On the basis of the assumed stress profiles, K_I solutions for an arbitrary point on the crack front were derived in [7] by an approximate analysis producing the following relation for a Mode I stress-intensity factor:

$$K_I(\bar{a}, \mathbf{q}) = M_f(\mathbf{q}) M_b(\mathbf{q}) k_t(p\bar{a}/4, \mathbf{q}) \frac{s\sqrt{p\bar{a}}}{p/2} \quad (2)$$

where M_f and M_b are front and back free-surface magnification factors, respectively, assumed to have the forms

$$\begin{aligned} M_f(\mathbf{q}) &= 1.43 - 0.24(\sin \mathbf{q} + \cos \mathbf{q}) \\ M_b(\mathbf{q}) &= 1.0 \end{aligned} \quad (3)$$

The parameter $k_t(r, \mathbf{q})$ is the local elastic stress concentration factor at a location (r, \mathbf{q}) from the origin (see Fig. 4), given by

$$k_t(r, \mathbf{q}) = 1 + (k_e - 1) \left(\frac{1}{1 + (\sin \mathbf{q} + \cos \mathbf{q})(r/r_i)} \right)^B \quad (4)$$

$$B = 2.70 - 2\sqrt{t/d} \quad (5)$$

where k_e is the elastic stress concentration factor at the origin which can be estimated by the Decock relation [8]

$$k_e = \frac{2 + 2(d/D)\sqrt{(dt)/(DT)} + 1.25(d/D)(D/T)}{1 + (t/T)\sqrt{(dt)/(DT)}} \quad (6)$$

where d and D are the mean diameters of the nozzle and vessel, respectively. A complete listing of the nomenclature used in Eqs. (2)-(6) is given in Appendix C.

The Guozhong and Qichao approximation [7] does not include the effects of cladding; therefore, finite-element solutions from the no-cladding cases in ORNL/TM-1999/159 were used for comparison. Figure 5a plots the maximum predicted K_I solutions as a function of flaw radius for both the ORNOZL/ABAQUS linear-elastic solutions (taken from [2] for the nocladding cases) and the results of the approximate analysis of Guozhong and Qichao [7] for the HFIR HB-2 nozzle corner geometry (see Appendix C). As indicated by Fig. 5b, the maximum deviation between the two solution sets was 7.7% for the smallest flaw size investigated with the ORNOZL/ABAQUS solution being higher than the Guozhong and Qichao estimate. These deviations fall within the $\pm 10\%$ uncertainty band established in ref. [7] using comparisons with published solutions for approximately 40 cracks from nine nozzle section geometries.

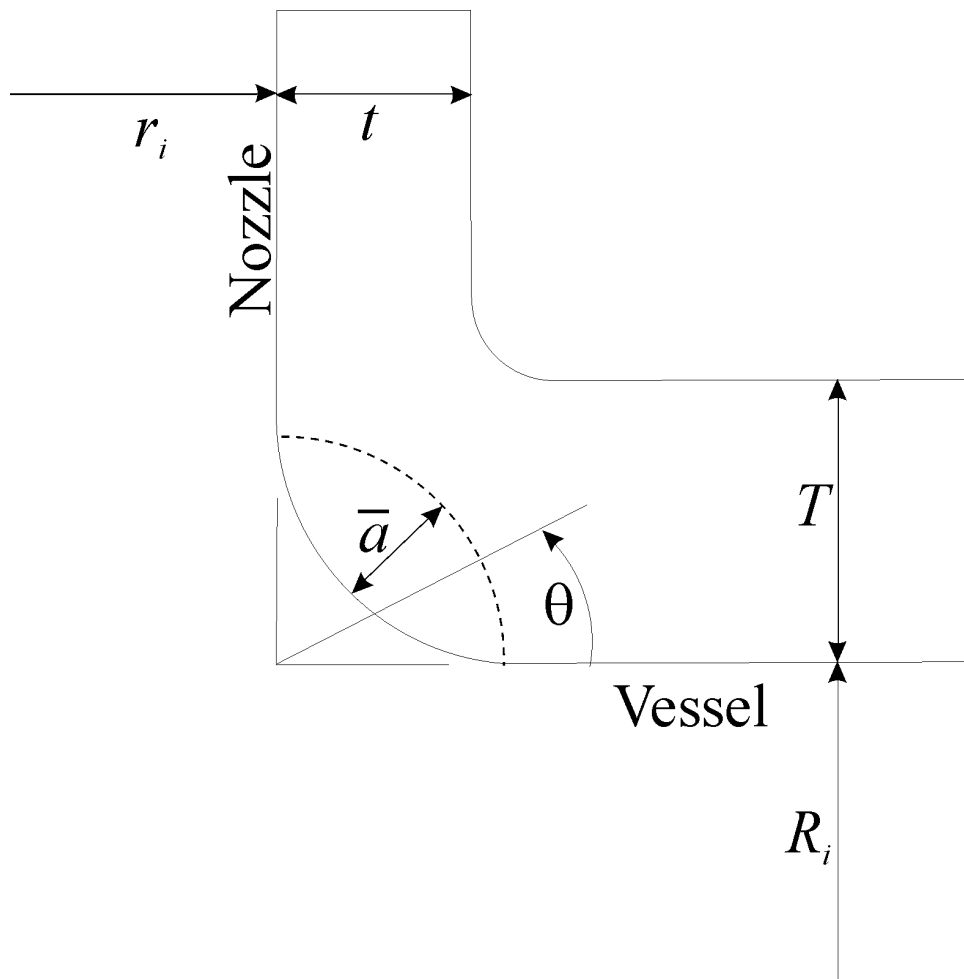
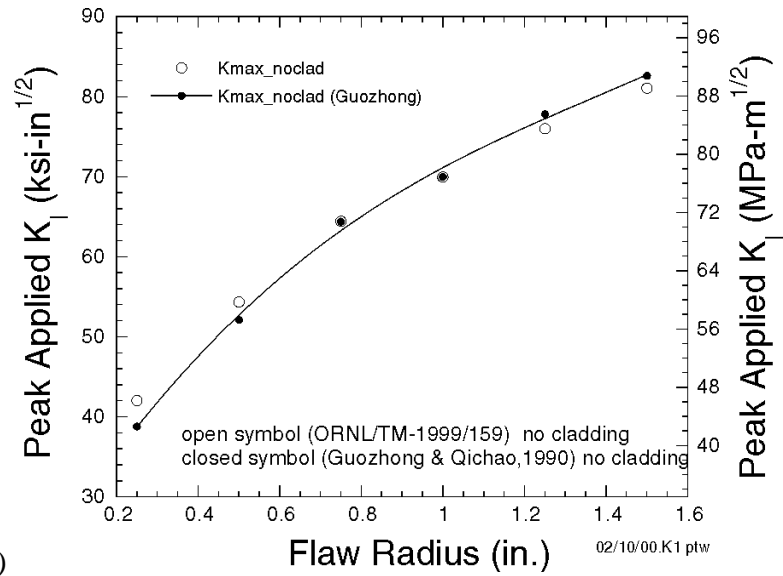
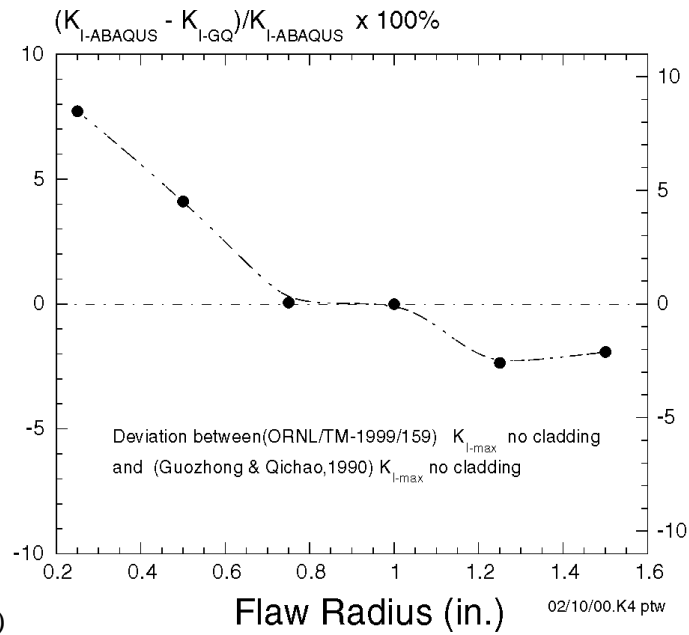


Fig. 4. Geometry of nozzle-corner flow.



(a)



(b)

Fig. 5. Comparison of ABAQUS solutions to predictions of Guozhong and Qichao (1990).

5. CONCLUSIONS

As a QA verification of the computer codes used in the report “Stress Intensity Factors for HFIR HB-2 Nozzle Corner” (ORNL/TM-1999/159) [2], benchmark problems have been solved that have established the following:

- The current version of the finite-element mesh generator code ORNOZL reproduces the results of the two sample problems given in its previously published user’s guide [4].
- The ABAQUS code reproduces, independently of ORNOZL, the results of a benchmark verification problem given in its Example Problems Manual that compares linear-elastic stress intensity factors for semi-elliptic surface flaws to solutions published in the literature [5,6].
- The ORNOZL/ABAQUS code combination was benchmarked against an approximate method [7] for estimating linear-elastic stress-intensity factors for corner flaws in pressure vessel nozzles.
- In addition, all input and output files produced during the analyses described in ORNL/TM-1999/159 have been archived on an electronic medium (CD-R74-ORNL/TM-1999/159) and transmitted to RRD personnel for archival storage.

REFERENCES

1. R. D. Cheverton and T. L. Dickson, *HFIR Vessel Life Extension with Enlarged HB-2 and HB-4 Beam Tubes*, ORNL/TM-13698, Lockheed Martin Energy Research, Oak Ridge Natl. Lab., December 1998.
2. P. T. Williams and B. R. Bass, "Stress Intensity Factors for HFIR HB-2 Nozzle Corner," ORNL/TM-1999/159, Oak Ridge National Laboratory, August 1999.
3. *ABAQUS Theory Manual, Version 5.7*, Hibbit, Karlson, and Sorenson, Inc., Providence, RI, 1997.
4. J. Keeney-Walker and B. R. Bass, *ORNOZL: A Finite-Element Mesh Generator for Nozzle-Cylinder Intersections Containing Inner-Corner Cracks*, NUREG/CR-5872 (ORNL/TM-11049), Martin Marietta Energy Systems, Inc., Oak Ridge Natl. Lab., September 1992.
5. *ABAQUS/Standard Example Problems Manual: Volume I*, Hibbit, Karlson, and Sorenson, Inc., Providence, RI, (1997) pp. 3.1.7-1 to 3.1.7-18.
6. J. C. Newman and I. S. Raju, "Stress-Intensity Factors for a Wide Range of Semi-Elliptical Surface Cracks in Finite Thickness Plates," *Engineering Fracture*
7. C. Guozhong and H. Qichao, "Approximate Stress-Intensity Factor Solutions for Nozzle Corner Cracks," *International Journal of Pressure Vessels and Piping* **42**, (1990) 75-96.
8. J. Decock, "Determination of Stress Concentrations Factors and Fatigue Assessment of Flush and Extruded Nozzles in Welded Pressure Vessels," *2nd International Conference on Pressure Vessel Tech., Part II*, ASME, San Antonio, Texas, Paper II-59, (1973) 821-834.

APPENDIX A: ORNOZL OUTPUT FILE (NOZZLE – I) CASE RUN: 11 FEBRUARY, 2000

```

o r n o z l   -   3   -   d   m e s h   g e n e r a t o r
o r n l       -   h s s t   p r o g r a m
d e c e m b e r   1 ,   1 9 8 4

```

NOZZLE TEST CASE 1

```

geometry type (isp)                = 4
crack profile (icrprf)             = 1
surface cladding option (iclad)    = 0
tip blunting option (iblt)        = 0
quarter or midside node option (itip) = 0
surface grid check option (modex)  = 0
crack face pressure (icfp)        = 0
adina version (iadina)            = 84
no. crack tip regions(2 or 3) (nreg) = 2

pressure vessel inside radius (pvr) = 343.000000
pressure vessel wall thickness (pvt) = 152.000000
nozzle inside radius (pnr)         = 114.000000
nozzle wall thickness (pnt)        = 102.000000
pressure vessel length (pvl)       = 1000.000000
nozzle total length (pnl)          = 1000.000000
nozzle inner fillet radius (r1)    = 38.000000
nozzle outer fillet radius (r2)   = 76.000000
nozzle length with thickness "pnt" (pnl1) = 670.000000
nozzle length from top to maximum thickness (pnl2) = 721.000000
nozzle maximum thickness (pnt2)   = 152.000000
number of crack elements(segments) on the crack front (ncrs) = 6
nozzle thickness for "itv" nozzles (pnt3) = 0.000000

```

finite element grid breakdown :

```

nx1      = 2
nx2      = 3
nx3      = 2
nx4      = 1
ny1      = 2
ny2      = 2
nz       = 6
size     = 5.00000
gradx    = 1.00000

```

crack definition parameters :

```

x direction (cra) =110.000000
y direction (crb) =110.000000

```

the computed stress intensity factors would correspond to the following elliptical angles

element number	theta (radians)	theta (degrees)	theta/(pi/2)
1	0.302E-01	0.173E+01	0.192E-01
2	0.242E+00	0.138E+02	0.154E+00
3	0.604E+00	0.346E+02	0.385E+00
4	0.967E+00	0.554E+02	0.615E+00
5	0.133E+01	0.762E+02	0.846E+00
6	0.154E+01	0.883E+02	0.981E+00

nozzle corner mesh parameters(generated):

```

case no. (indx1) = 2
r1 = 0.38000E+02
xsht = 0.10000E+03
ysht = 0.10000E+03

```

the computed stress intensity factors would correspond to the following elliptical angles

node number	theta (radians)	theta (degrees)	theta/(pi/2)		
1	0.000E+00	0.000E+00	0.000E+00	0.900E+02	0.707E+00
2	0.302E-01	0.173E+01	0.192E-01	0.883E+02	0.708E+00
3	0.604E-01	0.346E+01	0.385E-01	0.865E+02	0.709E+00
4	0.242E+00	0.138E+02	0.154E+00	0.762E+02	0.736E+00
5	0.423E+00	0.242E+02	0.269E+00	0.658E+02	0.783E+00
6	0.604E+00	0.346E+02	0.385E+00	0.554E+02	0.838E+00
7	0.785E+00	0.450E+02	0.500E+00	0.450E+02	0.889E+00
8	0.967E+00	0.554E+02	0.615E+00	0.346E+02	0.933E+00
9	0.115E+01	0.658E+02	0.731E+00	0.242E+02	0.967E+00
10	0.133E+01	0.762E+02	0.846E+00	0.138E+02	0.989E+00
11	0.151E+01	0.865E+02	0.962E+00	0.346E+01	0.999E+00
12	0.154E+01	0.883E+02	0.981E+00	0.173E+01	0.100E+01
13	0.157E+01	0.900E+02	0.100E+01	0.000E+00	0.100E+01

angular division - nozzle

div	angle
1	0.00000
2	1.25689
3	2.51378
4	3.77067
5	5.02756
6	7.54134
7	10.05512
8	14.17148
9	18.28785
10	22.04923
11	25.81061
12	30.88520
13	35.95980
14	45.69245
15	55.42510
16	72.71255
17	90.00000

angular division - vessel

div	angle
1	0.83525
2	15.69604
3	30.55683
4	45.41762
5	60.27842
6	75.13921
7	90.00000

mesh generation parameters - subroutine revol v :

```

in = 3
iv = 3
ix = 5
iy = 9
icf = 11
ist = 5
indx1 = 2
nx = 25
ny = 13
nz1 = 3
nz2 = 3
nz3 = 0
nozshp = 2

```

perturbation vector for crack front nodes

node	d1	d2	d3
1	0.100000E+01	0.000000E+00	0.000000E+00
2	0.100000E+01	0.000000E+00	0.000000E+00
3	0.100000E+01	0.000000E+00	0.000000E+00
4	0.977101E+00	0.212778E+00	0.000000E+00
5	0.910891E+00	0.412647E+00	0.000000E+00
6	0.822262E+00	0.569109E+00	0.000000E+00
7	0.707107E+00	0.707107E+00	0.000000E+00
8	0.569106E+00	0.822264E+00	0.000000E+00
9	0.412650E+00	0.910890E+00	0.000000E+00
10	0.212774E+00	0.977101E+00	0.000000E+00
11	0.000000E+00	0.100000E+01	0.000000E+00
12	0.000000E+00	0.100000E+01	0.000000E+00
13	0.000000E+00	0.100000E+01	0.000000E+00

number of nodes in adina crack model. . . . (nod)= 2616
number of crack tip elements.(nelt)= 96
first element on crack front.(nre2)= 49
first element of outer region(nre3)= 0
number of regular elements.(nel)= 408
number of internal pres elements(nprel)= 218
number of crack face pres elements (nprcf)= 0

APPENDIX B: ORNOZL OUTPUT FILE (NOZZLE – II) CASE RUN: 11 FEBRUARY, 2000

```

o r n o z l   -   3   -   d   m e s h   g e n e r a t o r
o r n l       -   h s s t   p r o g r a m
d e c e m b e r   1 ,   1 9 8 4

```

NOZZLE TEST CASE 1

```

geometry type (isp)                = 4
crack profile (icrpf)              = 1
surface cladding option (iclad)    = 0
tip blunting option (iblt)        = 0
quarter or midside node option (itip) = 0
surface grid check option (modex)  = 0
crack face pressure (icfp)        = 0
adina version (iadina)            = 84
no. crack tip regions(2 or 3) (nreg) = 2

pressure vessel inside radius (pvr) = 343.000000
pressure vessel wall thickness (pvt) = 152.000000
nozzle inside radius (pnr)         = 114.000000
nozzle wall thickness (pnt)        = 102.000000
pressure vessel length (pvl)       = 1000.000000
nozzle total length (pnl)          = 1000.000000
nozzle inner fillet radius (r1)    = 38.000000
nozzle outer fillet radius (r2)    = 76.000000
nozzle length with thickness "pnt" (pnl1) = 670.000000
nozzle length from top to maximum thickness (pnl2) = 721.000000
nozzle maximum thickness (pnt2)    = 152.000000
number of crack elements(segments) on the crack front (ncrs) = 6
nozzle thickness for "itv" nozzles (pnt3) = 0.000000

```

finite element grid breakdown :

```

nx1    = 2
nx2    = 3
nx3    = 2
nx4    = 1
ny1    = 2
ny2    = 2
nz     = 6
size   = 5.00000
gradx  = 1.00000

```

crack definition parameters :

```

x direction (cra) =110.000000
y direction (crb) =110.000000

```

the computed stress intensity factors would correspond to the following elliptical angles

element number	theta (radians)	theta (degrees)	theta/(pi/2)
1	0.302E-01	0.173E+01	0.192E-01
2	0.242E+00	0.138E+02	0.154E+00
3	0.604E+00	0.346E+02	0.385E+00
4	0.967E+00	0.554E+02	0.615E+00
5	0.133E+01	0.762E+02	0.846E+00
6	0.154E+01	0.883E+02	0.981E+00

nozzle corner mesh parameters(generated):

```

case no. (indx1) = 2

```

```

r1          = 0.38000E+02
xsht       = 0.10000E+03
ysht       = 0.10000E+03

```

the computed stress intensity factors would correspond to the following elliptical angles

node number	theta (radians)	theta (degrees)	theta/(pi/2)		
1	0.000E+00	0.000E+00	0.000E+00	0.900E+02	0.707E+00
2	0.302E-01	0.173E+01	0.192E-01	0.883E+02	0.708E+00
3	0.604E-01	0.346E+01	0.385E-01	0.865E+02	0.709E+00
4	0.242E+00	0.138E+02	0.154E+00	0.762E+02	0.736E+00
5	0.423E+00	0.242E+02	0.269E+00	0.658E+02	0.783E+00
6	0.604E+00	0.346E+02	0.385E+00	0.554E+02	0.838E+00
7	0.785E+00	0.450E+02	0.500E+00	0.450E+02	0.889E+00
8	0.967E+00	0.554E+02	0.615E+00	0.346E+02	0.933E+00
9	0.115E+01	0.658E+02	0.731E+00	0.242E+02	0.967E+00
10	0.133E+01	0.762E+02	0.846E+00	0.138E+02	0.989E+00
11	0.151E+01	0.865E+02	0.962E+00	0.346E+01	0.999E+00
12	0.154E+01	0.883E+02	0.981E+00	0.173E+01	0.100E+01
13	0.157E+01	0.900E+02	0.100E+01	0.000E+00	0.100E+01

angular division - nozzle

div	angle
1	0.00000
2	1.25689
3	2.51378
4	3.77067
5	5.02756
6	7.54134
7	10.05512
8	14.17148
9	18.28785
10	22.04923
11	25.81061
12	30.88520
13	35.95980
14	45.69245
15	55.42510
16	72.71255
17	90.00000

angular division - vessel

div	angle
1	0.83525
2	15.69604
3	30.55683
4	45.41762
5	60.27842
6	75.13921
7	90.00000

mesh generation parameters - subroutine revolv :

```

in          = 3
iv          = 3
ix          = 5
iy          = 9
icf        = 11
ist        = 5
indx1      = 2
nx         = 25
ny         = 13
nz1        = 3
nz2        = 3
nz3        = 0
nozshp     = 2

```

perturbation vector for crack front nodes

node	d1	d2	d3
1	0.100000E+01	0.000000E+00	0.000000E+00
2	0.100000E+01	0.000000E+00	0.000000E+00
3	0.100000E+01	0.000000E+00	0.000000E+00
4	0.977101E+00	0.212778E+00	0.000000E+00
5	0.910891E+00	0.412647E+00	0.000000E+00
6	0.822262E+00	0.569109E+00	0.000000E+00
7	0.707107E+00	0.707107E+00	0.000000E+00
8	0.569106E+00	0.822264E+00	0.000000E+00
9	0.412650E+00	0.910890E+00	0.000000E+00
10	0.212774E+00	0.977101E+00	0.000000E+00
11	0.000000E+00	0.100000E+01	0.000000E+00
12	0.000000E+00	0.100000E+01	0.000000E+00
13	0.000000E+00	0.100000E+01	0.000000E+00

number of nodes in adina crack model. . . . (nod)= 2616
number of crack tip elements.(nelt)= 96
first element on crack front.(nre2)= 49
first element of outer region(nre3)= 0
number of regular elements.(nel)= 408
number of internal pres elements(npres)= 218
number of crack face pres elements(nprcf)= 0

**APPENDIX C MATHCAD DATA SHEETS WITH EVALUATION OF
APPROXIMATE STRESS-INTENSITY FACTORS USING THE
GUZHONG AND QICHAO (1990) APPROXIMATION**

Project: HFIR Vessel Life Extension

SHEET 1 OF 7

Report. No: ORNL/TM-2000/70

Calculation by: P. T. Williams, Ph.D., P.E.

Date: 04 February 2000

Reference

1. C. Guozhong and H. Qichao, "Approximate Stress-Intensity Factor Solutions for Nozzle Corner Cracks," *International Journal of Pressure Vessels and Piping* **42**, (1990) 75-96.

Geometry Data (inches)

$$\begin{aligned}
 a &:= 0.5 & d &:= 20.0 \\
 r_i &:= 7.0 & D &:= 97.375 \\
 t &:= 6.0 & \theta &:= 0, 2 \dots 90 \\
 T &:= 3.125 & &
 \end{aligned}$$

vessel Hoop Stress (ksi)

$$\sigma := 13.986$$

Stress Concentration Factor Model

Decock's (1973) Equation for Elastic Concentration Factor
 J. Decock, "Determination of Stress Concentration Factors and Fatigue Assessment of Flush and Extruded Nozzles in Welded Pressure Vessels," *Conf. Pres. Ves. Technol.*, Part II, (1973) 821-834.

$$k_e := \frac{\left[2.0 + 2.0 \cdot \left(\frac{d}{D} \right) \cdot \sqrt{\frac{(d \cdot t)}{(D \cdot T)}} + 1.25 \cdot \left(\frac{d}{D} \right) \cdot \left(\frac{D}{T} \right) \right]}{1.0 + \left(\frac{t}{T} \right) \cdot \sqrt{\frac{(d \cdot t)}{(D \cdot T)}}}$$

$$k_e = 4.651$$

Stress Concentration Factor at (r,θ)

$$B := 2.7 - 2 \cdot \sqrt{\frac{t}{d}}$$

$$B = 1.605$$

$$k_t(x,y) := 1 + (k_e - 1) \cdot \left[\frac{1}{1 + \frac{\pi \cdot x}{4.0 \cdot r_i} \cdot \left(\sin\left(y \cdot \frac{\pi}{180}\right) + \cos\left(y \cdot \frac{\pi}{180}\right) \right)} \right]^B$$

Local Stress-Intensity Factor (ksi $\sqrt{\text{in}}$)

$$K_I(x, y) := \left[1.43 - 0.24 \cdot \left(\sin\left(y \cdot \frac{\pi}{180}\right) + \cos\left(y \cdot \frac{\pi}{180}\right) \right) \right] \cdot (\sigma \cdot k_t(x, y)) \cdot \frac{2 \cdot \sqrt{\pi x}}{\pi}$$

Stress-Intensity Factor for $r_f = 1.5$ in.

$$a := 1.23$$

$\theta =$	$k_t(a, \theta) =$	$K_I(a, \theta) =$	$k_t(a, \theta) \cdot \sigma =$
0	3.967	82.620	55.479
2	3.947	81.641	55.204
4	3.928	80.708	54.941
6	3.910	79.820	54.692
8	3.894	78.978	54.455
10	3.878	78.180	54.231
12	3.862	77.428	54.020
14	3.848	76.721	53.821
16	3.835	76.058	53.636
18	3.823	75.440	53.462
20	3.811	74.867	53.302
22	3.800	74.339	53.154
24	3.791	73.855	53.018
26	3.782	73.415	52.895
28	3.774	73.020	52.784
30	3.767	72.668	52.686
32	3.761	72.361	52.600
34	3.756	72.098	52.526
36	3.751	71.879	52.465
38	3.748	71.703	52.416
40	3.745	71.572	52.379
42	3.743	71.484	52.355
44	3.742	71.440	52.343
46	3.742	71.440	52.343

Stress-Intensity Factor for $r_f = 1.25$ in.

$$a := 1.043$$

$\theta =$	$k_I(a, \theta) =$	$K_I(a, \theta) =$	$k_I(a, \theta) \cdot \sigma =$
0	4.057	77.805	56.737
2	4.039	76.933	56.491
4	4.022	76.100	56.257
6	4.006	75.307	56.034
8	3.991	74.553	55.823
10	3.977	73.839	55.622
12	3.963	73.164	55.433
14	3.951	72.530	55.255
16	3.939	71.934	55.088
18	3.928	71.379	54.932
20	3.917	70.863	54.787
22	3.908	70.387	54.654
24	3.899	69.951	54.532
26	3.891	69.554	54.421
28	3.884	69.197	54.321
30	3.878	68.880	54.232
32	3.872	68.603	54.154
34	3.867	68.365	54.088
36	3.863	68.167	54.032
38	3.860	68.008	53.988
40	3.858	67.889	53.955
42	3.856	67.810	53.932
44	3.855	67.770	53.921
46	3.855	67.770	53.921

Stress-Intensity Factor for $r_f = 0.75$ in.

$$a := 0.647$$

$\theta =$	$k_t(a, \theta) =$	$K_I(a, \theta) =$	$k_t(a, \theta) \cdot \sigma =$
0	4.262	64.387	59.614
2	4.250	63.760	59.444
4	4.239	63.160	59.282
6	4.228	62.586	59.127
8	4.217	62.039	58.979
10	4.207	61.520	58.839
12	4.198	61.028	58.707
14	4.189	60.564	58.581
16	4.180	60.128	58.464
18	4.172	59.721	58.354
20	4.165	59.341	58.252
22	4.158	58.991	58.157
24	4.152	58.669	58.070
26	4.146	58.376	57.991
28	4.141	58.112	57.920
30	4.137	57.877	57.857
32	4.133	57.671	57.801
34	4.129	57.494	57.754
36	4.127	57.347	57.714
38	4.124	57.229	57.682
40	4.123	57.141	57.658
42	4.121	57.082	57.643
44	4.121	57.052	57.635
46	4.121	57.052	57.635

Stress-Intensity Factors for $r_f = 0.5$ in.

$$a := 0.397$$

$\theta =$	$k_I(a, \theta) =$	$K_I(a, \theta) =$	$k_I(a, \theta) \cdot \sigma =$
0	4.404	52.113	61.596
2	4.396	51.659	61.484
4	4.388	51.223	61.377
6	4.381	50.806	61.275
8	4.374	50.408	61.177
10	4.367	50.029	61.084
12	4.361	49.669	60.996
14	4.355	49.329	60.912
16	4.350	49.010	60.834
18	4.344	48.710	60.760
20	4.339	48.431	60.692
22	4.335	48.173	60.629
24	4.331	47.936	60.570
26	4.327	47.719	60.517
28	4.324	47.524	60.470
30	4.321	47.350	60.427
32	4.318	47.198	60.390
34	4.316	47.067	60.358
36	4.314	46.958	60.331
38	4.312	46.871	60.309
40	4.311	46.805	60.293
42	4.310	46.761	60.283
44	4.310	46.740	60.277
46	4.310	46.740	60.277

Stress-Intensity Factor for $r_f = 0.25$ in.

$$a := 0.209$$

$\theta =$	$k_t(a, \theta) =$	$K_I(a, \theta) =$	$k_t(a, \theta) \cdot \sigma =$
0	4.517	38.784	63.180
2	4.513	38.478	63.118
4	4.509	38.184	63.058
6	4.505	37.902	63.001
8	4.501	37.632	62.947
10	4.497	37.375	62.895
12	4.493	37.131	62.845
14	4.490	36.900	62.798
16	4.487	36.682	62.754
18	4.484	36.478	62.713
20	4.481	36.288	62.675
22	4.479	36.112	62.639
24	4.476	35.949	62.606
26	4.474	35.801	62.576
28	4.472	35.668	62.549
30	4.471	35.549	62.525
32	4.469	35.444	62.504
34	4.468	35.355	62.486
36	4.467	35.280	62.471
38	4.466	35.220	62.458
40	4.465	35.175	62.449
42	4.465	35.145	62.443
44	4.464	35.130	62.440
46	4.464	35.130	62.440

Nomenclature

a = flaw depth

R_i = vessel inner radius

r_i = nozzle inner radius

t = nozzle wall thickness

T = vessel wall thickness

d = mean nozzle diameter

D = mean vessel diameter

σ = vessel hoop stress

θ = flaw front angle

k_e = elastic concentration factor

k_t = local stress concentration factor

B = exponent for k_t

K_I = local applied stress intensity factor

INTERNAL DISTRIBUTION

1. B. R. Bass
2. S. E. Burnette
3. R. D. Cheverton
4. S. J. Chang
5. K. W. Childs
6. D. H. Cook
7. T. L. Dickson
8. D. M. Hetrick
- 9-11. J. R. Inger
12. S. K. Iskander
13. M. A. Kuliasha
14. W. J. McAfee
15. L. D. Proctor
16. D. L. Selby
- 17-20. P. T. Williams
21. Research Reactors Division – DCC – RC
22. ORNL Patent Office
- 23-24. Central Research Library
- 25-26. Laboratory Records (for OSTI)
27. Laboratory Records, RC